

Improvement of butt-fusion welding procedure and performance evaluation method for thick-walled bimodal polyethylene pipes

Zhenchao Wang^{a,b}, Shijun Zhang^b, Jichun Qie^b, Qijiang You^b, Lu Xu^b, Qiuju Zhang^{a,*}

^a School of Mechanical Engineering, Jiangnan University, Wuxi, 214122, China

^b Rothenberger (Wuxi) Pipe Technologies Co., Ltd., Wuxi, 214161, China

ARTICLE INFO

Keywords:

HDPE pipe
Butt fusion welding
Welding procedure
Welding interface
Performance testing

ABSTRACT

High-density polyethylene (HDPE) pipes have been continuously improved by the progress made by the resin industry and pipe manufacturers. Together with the advanced technology of welding equipment in terms of structure reliability and automations, HDPE pipes have been gradually applied to higher pressure level, bigger diameter, and thicker walls in operations which have become the preferred piping system for nuclear safety application in transporting cooling seawater. There are substantial differences in parameter settings when applying heat and force during different welding procedures, as well as the complicated evaluation methods for mechanical properties, which causes communication barriers between engineers and researchers. Thus, it is necessary to comprehensively study the welding procedures and evaluation methods to standardize the evaluation protocols in the industry. In this paper, based on the assumptions of temperature effect and molecular chain diffusion dynamics at the welding interface, the optimization of the welding procedure is proposed. Some well-established evaluation methods have been used for performance assessment and their feasibilities are discussed. The idea of creating crack along the weld interface is adopted as new method to evaluate the material ability of fracture resistance. Specimens with unilateral notch and weld interface crack are proposed and subjected for quasi-static axial tensile test. The fracture stress and fracture energy at the welding interface are used to differentiate the quality of the joint from different welding procedures. The fracture morphologies of the weld interface are analyzed. A complete picture is drawn for the mechanical fracture resistance of the weld interface. The method used in this paper can be correlated to the pipeline design conditions, therefore could be applied to the real-time engineering applications. Moreover, the evaluation method proposed in this paper is simple, reliable, and easy to implement.

1. Introduction

Polyethylene (PE) is the most widely used polyolefin, accounting for 29 % global synthetic polymer production. Polyethylene materials are indispensable in people's daily lives nowadays [1]. There are hundreds of different grades of polyolefins commercialized with a wide variety of material properties. Various metal catalysts can tailor the polymerization states that control the key material parameters, such as molecular weight and molecular weight distribution [2]. Bimodal polyethylene is a blend of linear polyethylene and branched polyethylene, with a low-molecular-weight homopolymer folding the molecular chain neatly into the crystalline area for the material strength, good processing ability and elongation property. The copolymer part participates in crystallization and becomes a "tie molecule" through the crystal area,

ensuring high toughness and mechanical crack resistance [3,4]. At the same time, bimodal polyethylene embodies the respective advantages of low molecular weight and high molecular weight, not only has good extrusion performance, but also has very good anti-"sagging" performance, which lift the limitation of polyethylene material processing into large-diameter pipes, and the current extrusion thick-walled pipes can reach a diameter of more than 2500 mm or wall thickness of 100 mm [5]. Bimodal polyethylene has excellent resistance to slow crack growth (SCG), and the operating temperature has been increased from room temperature to 60 °C. This makes it the preferred material for pipes used in the high safety level nuclear power plants, especially for large-diameter pressurized pipes that transport seawater for cooling [6].

The most commonly used pipe connection method is the butt-fusion welding that can make the joint meeting or exceeding the mechanical

* Corresponding author.

E-mail address: qjzhang@jiangnan.edu.cn (Q. Zhang).

<https://doi.org/10.1016/j.polytest.2024.108448>

Received 13 February 2024; Received in revised form 26 April 2024; Accepted 9 May 2024

Available online 10 May 2024

0142-9418/© 2024 The Authors. Published by Elsevier Ltd. This is an open access article under the CC BY-NC-ND license (<http://creativecommons.org/licenses/by-nc-nd/4.0/>).

properties of the bulk material which is much desired in the large-diameter thick-walled piping. In particular, the well-known standard of American Society of Mechanical Engineers (ASME) only allows the use of butt fusion welding connections for nuclear-safe grade polyethylene buried pipes [7]. However, the welding performance of polyethylene pipes is affected by a variety of factors. The temperature and pressure applied during the fusion process can affect the performance of the fusion joint [8,9]. The welding process leads to a change in the molecular chain orientation of the polymer in the welding region, which affects the welding performance [10–12]. The viscosity and interaction forces of molten material at the weld interface affect the quality of the weld interface [13]. Tensile and rapid cooling of polyethylene melt affect crystallization behavior [14]. The tensile failure of the polymer interface is related to the welding time [15]. The deposition of a kind of powder at the weld interface can change the interface connection [16]. In addition, defects, welding bead, and stress concentrations introduced during the fusion process can also affect the performance of the fusion joint [17–19].

Fabian et al. [5] pointed out that brittle failure occurred at the welds of some thick-walled pipes, which led to a sense of uncertainty of using thick-walled pipes in the industry and customers. At the same time, the welding parameters for the thick-walled PE given in the DVS (Deutscher Verband für Schweißen und verwandte Verfahren e.V.) [20] guidelines are extrapolated. At present, there is a lack of systematic experimental studies on wall thicknesses above 30 mm. Tarek et al. [21–23] investigated the effects of butt fusion welding process and specimen thickness on the fracture toughness of polyethylene pipes, resulted that the fracture toughness of all welded specimens was lower than that of the bulk material, and the fracture toughness of the material was decreased with the increase of the thickness of the specimen. Kalyanam et al. [6] found that the Pennsylvania Notch Test (PENT) for SCG resistance of welded joints under ASME system was only thousandth of that of bulk materials. Therefore, it is necessary to conduct in-depth research on butt fusion welding process to better understand the polymer welding physics, especially for bimodal polyethylene pipes with large diameter and thick wall [24].

At present, different countries in the world use different welding procedures for butt-fusion welding of PE pipes. Based on the process pressure and temperature, those procedures are summarized as three main types, namely a Single Low Pressure procedure (i.e., SLP, used by most countries, such as Germany DVS 2207–1, UK gas pipe GIS/PL2-3 [25] and smaller diameter water pipe WIS 4-32-8 [26], China GB/T 32,434 [27]), Single High Pressure procedure (i.e., SHP, mainly used in the United States, ASTM F2620 [28]), The Dual Low Pressure procedure (DLP, mainly used in larger diameter water pipes in the UK, WIS 4-32-8). These welding procedures are included in ISO 21307:2017 [29] as three standard procedures.

There are several ways to evaluate the reliability of short-term mechanical properties for the effectiveness of these welding procedures. Validation of the ASTM F2620 procedure requires rapid tensile impact test indicated in ASTM F2634 [30], as well as manual flexure test [28]. WIS 4-32-08 requires the use of waist specimens for tensile test. The DVS system requests tensile test of DVS 2203–2 [31], and flexure test of DVS 2203–5 [32], together with the test indicators specified in DVS 2203–1 [33]. ISO 21307 requires tensile test of ISO 13953 [34] and rapid tensile impact test of ASTM F2634. The EU standard recommends flexure test of EN 12814–1 [35], tensile strength test of EN 12814–2 [36], and the breaking energy test of EN 12814–7 [37]. The evaluation method is crucial for ensuring correct judgement of the performance from welding procedures. They have already been studied over the years, and a variety of methods have been developed. The most commonly used method is tensile test [38–41].

Noted that the current researches on the butt-fusion welding performance of PE pipes are mainly based on the empirical study of structural reliability. The tensile specimens used can be divided into two categories. The first one is the specimen with a long parallel section at

the joint. Accordingly, there is no stress concentration at the joint caused by the shape of the specimen. The second is the waisted specimen with a tapering arc at the joint, which produces stress concentration at the waisted area. The specimens from EN 12174–7 and EN 12174-2 Annex C have a large stress concentration due to the small radius of the waist arc ($r = 5$ mm), which can ensure the fracture occur at the weld joint.

Mike et al. [42] has used a variety of mechanical test methods to study the performance of contaminated butt-fusion joints in PE pipes. They found that some test methods were too poor to distinguish their quality, such as three-point flexure test, tensile test using a dumbbell specimen, the tensile impact test with an evaluation of breaking energy and a high-temperature hydrostatic pressure test. Above mentioned tests were unable to produce failures at the joint, resulted highly discrete test data. According to them, the most discriminating short-term performance test was a tensile test using a thin waist specimen which could ensure that the fracture occur at the joint not at the bulk material. Moreover, they suggested that only the fracture energy value could be used to distinguish the fracture condition of joints. The same view was held by Muhammad, Kim and Tarek et al. [43–45].

The authors also strongly agree the use of thin waist specimens to evaluate fracture toughness through fracture energy. This method has been used by authors to test the welding character located at different points of wall thickness. However, the authors believe that there is a great disadvantage when using thin waist specimens to evaluate the performance of different welding procedures. The reason is that the width and shape of the molten zone (MZ) and the heat-affected zone (HAZ) at the joint are varied due to the differences of the shape and size of the joint created by thermo-mechanical coupling affected by welding procedures. The stress concentrations are different with specific locations in the joint which would be represented by the specimen prepared from the specific joints.

The authors propose a new evaluation method in the paper. The purpose is to ensure fractures occur on weld interface by applying high stress concentrations. Therefore, the mechanical properties of the joint are characterized by evaluating the welded interface not the whole welded zone. This method can evaluate different welding procedures, as well as evaluate the influence of welding defects or environmental factors on the performance of welded interface. With this method, the fracture mechanics can be used to relate the experimental results to the allowed form and size of defects when considering short-term mechanical properties in pipeline design. Tarek et al. have used a notched pipe ring segment to perform a three-point bending test to analyze the radial fracture toughness of welded and unwelded materials by the principle of fracture mechanics [23].

Except the tensile test, some other methods were reported for assessing the property of butt-fusion welded joints, such as the hydraulic axial tensile tests using entire pipes as specimens [46], the shaker table tests to check the effect of vibration on the joint [47], and the nano-indentation tests to characterize the creep properties of joints [48]. These methods have enriched the researcher horizons and provided more possibilities to delve into the performance of weld joints.

The performance of the butt-fusion joint is affected not only by the welding process parameters, but also by the welding equipment, the operators and the operating environment. In order to avoid these influencing factors, three units of fully automatic welding equipment were specially designed and manufactured in accordance with the provisions of ISO12176 [49]. These welding equipment were used to carry out the welding operations in the room environment.

The poor distributive mixing of carbon black masterbatch will have an impact on the mechanical properties of the pipe as well as welded joint [50–52]. In order to avoid its influence, the commercialized polyethylene compound which complies to the requirement of ISO 4427–1 [53] is selected and the pipe is also produced in accordance with standard ASTM F 714 [54] by professional extrusion equipment.

The presence of the welding bead has potential impact on the performance of the welded joint. Haroon [55] conducted a thin film tensile

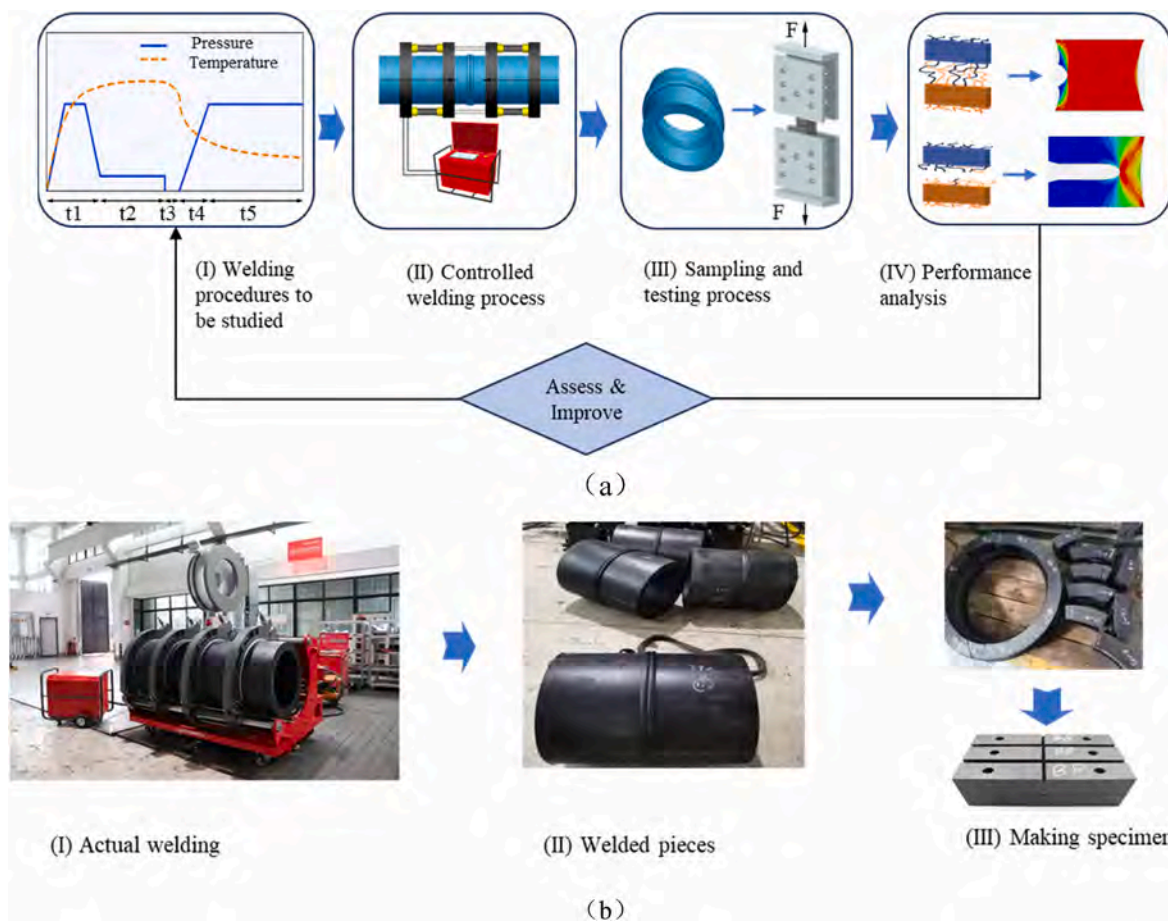


Fig. 1. Graphical overview and sampling process (a) A schematic overview of the study process and method. (b) The actual photos of welding process and specimens.

test and found that the initial deformation of the specimen with bead occur in the center of the molten zone (MZ), but the final failure occurred at the junction of the weld bead and the bulk material. For the film tested without bead, both the maximum deformation and rupture occurred in the center of the MZ. This was due to the stress concentration caused by pseudo notches created by the bead edges. Generally, the presence of the bead increases the stress concentration at the joint by 30 % [43]. Some researchers believed that removing the bead could clearly characterize the performance of the weld joint [44]. At the same time, it is uncertain whether the bead shall be retained or removed in real operations. This article aims to analyze the performance of the weld interface and will remove the effects of bead in the new method in order to better discuss the effects of the welding procedures.

2. Experiment

2.1. Materials

The bimodal PE compound coded as Borstar HE3490-ELS-H (Borouge Pte Ltd, UAE) is selected. In which the PE accounts for more than 97.5 %, the content of carbon black is 2.3 % and its dispersion meets the requirement of ISO 4427-1. The outer diameter of the pipe is 812.8 mm and the wall thickness is 74 mm (produced by Chinaust Group with Battenfeld-Cincinnati single screw extruder), which complies to the standard of ASTM F714.

2.2. Welding equipment

Three welding machines were designed by the authors to conduct the welding procedures automatically. They are capable of presetting the

parameters and executing the required procedures. Those machines were manufactured by Rothenberger Wuxi (a Germany company operated in China). Those machines also comply to the standard of ISO 12176. Welding of SHP is conducted by one machine called R1000CF SHP. Welding of SLP and New P are conducted by another machine named R1000CF SLP. The interface crack specimens and temperature measures are done by a small machine coded R110CF.

2.3. Welding procedures

The welding procedure refers to the process of applying required heat and force on the pipe ends to form a welding joint. The diagrams of the studied procedures can be seen in section 3.2.1. Some critical parameters are as follows. The heat soaking time is in the second (s), and the pipe wall thickness e_n is in millimeters (mm).

For SHP, the procedure specified in ASTM F2620-2020 and ISO 21307-2017, the temperature of heating plate is set at 215 °C, the heat soaking time is set as $11 \times e_n$ and the net interfacial pressure is set as 0.52 MPa.

For SLP, the procedure specified in ISO 21307, the temperature of heating plate is set at 225 °C, the heat soaking time is set as $13.5 \times e_n$ and the net interfacial pressure is set as 0.17 MPa.

For NEW P, means the proposed welding procedure, the temperature of heating plate is set at 250 °C, the heat soaking time is set as $13.5 \times e_n$ and the net interfacial pressure is set as 0.05 MPa.

The BASE refers to the unwelded material of the pipe, also called as bulk material in the paper, which serves as a benchmark for welded material.

2.4. Testing

2.4.1. Mechanical property test

2.4.1.1. Specimens with unilateral notch. Six specimens are extracted evenly around each studied joint for each test category. Unilateral V-shaped notch is machined to ensure the center line of V notch pass through the welding interface and be perpendicular to the long axis of the specimen. Neutral coolant is sprayed throughout the process to avoid heat influence. More information can be found in chapter 3.

2.4.1.2. Specimens with weld interface crack. During the welding process, thin iron sheet is placed and fixed in the center of the fusion interface to create surface crack. Six specimens are made for each test category. More information can be found in section 3.

2.4.1.3. Specimens with circular notch for morphology study. Circular V-shaped notch is machined to ensure the center line of V notch pass through the welding interface and be perpendicular to the long axis of the round bar specimen. More information can be found in section 3.

2.4.1.4. Axial tensile tests. The tensile tests are carried out after the specimens conditioned at 20 ± 2 °C for 12 h. Universal tensile testing machines are used. More information can be found in section 3.

2.4.2. Physicochemical analysis

The Rotational Rheometer (RR), Differential Scanning Calorimetry (DSC), Oxidative Induction Test (OIT) and Fourier Transform Infrared Spectroscopy (FTIR) are used for chemical character analysis.

3. Results and discussions

3.1. Theoretical analysis

3.1.1. Graphical overview of the study

Fig. 1(a) is a graphical overview of the research process and methods used in this paper. The research process includes welding, sample preparation, testing, and performance analysis, followed by improvements to the welding procedure. Importantly, the welding procedure is automatically executed and controlled by specially designed welding equipment. And the mechanical properties are assessed by multiple methods. Fig. 1(b) are the actual photos showing that the pipe pieces with outer diameter of 812.8 mm and wall thickness of 74 mm are welded and some of the test specimens are made.

3.1.2. Thermo-mechanical coupling effect

The essence of polymer welding is that the molecular chains stretch under the action of heat, diffuse and entangle each other, and crystallize to form a new molecular chain structure during the cooling process. Kim and Wool [56] described the interdiffusion process at the polymer-polymer interface using the behavior of small chains and small enveloped chain ball. Polymer chain diffusion increases with time and is also related to molecular weight, as is shown $(t) \approx \frac{1}{t^2 M^{-1/2}}$, where $l(t)$ is the average diffusion depth, M is the molecular weight, and t is the contact diffusion time. $l(t)$ is positively correlated with chain unwinding and pulling out, which determines the mechanical properties of the polymer.

According to the molecular chain diffusion model, diffusion time and molecular weight are important parameters. Higher fusion temperatures maintain long diffusion times and provide higher heat energy to drive greater molecular weight diffusion. In addition, in the welding process, it is necessary to apply the welding force that create large amount of energy to encourage the diffusion of the molecular chains and to prevent cracks and voids caused by the expansion and contraction of the material during the crystallization process. However, the greater welding

force can extrude the molten material out of the weld area, resulting in less melted material at the weld interface for the polymer molecule diffusion and entanglement. Therefore, obtaining an optimal thermodynamic coupling state can promote the activity of the molecular chain and increase the depth of diffusion for good mechanical properties at the welding interface.

3.1.3. Mechanical property evaluation methods

Before the polymer chain breaks, all the covalent bonds in the polymer chain in front of the crack are stretched close to the limit of elongation. The breaking of the polymer chain breaks only one covalent bond in the polymer chain but dissipates the elastic energy stored in all the bonds in the polymer chain. That is, when it breaks, the anterior fibers are destroyed, releasing all the elastic energy in the fibers around the crack tip [57]. If the crack tip has a strong softening ability, the toughness and fatigue threshold of the polymer will be increased [58]. It is conceivable that the tensile fracture of polymers should be the result of the rupture or untying of its interfacial molecular chains. Therefore, the diffusion, entanglement and crystallization of molecular chains at the polymer welding interface will affect its fracture properties.

The establishment of the mechanical constitutive model of semi-crystalline materials generally requires short-term and long-term performance evaluation. Short-term properties are generally analyzed by tensile stress and deformation. The stress-strain curve is used to obtain information of yield strength, tensile strength, and modulus, which are used to determine material's ductility or brittleness. This method is also used to analyze the properties of welded joints. However, due to the continuous improvement of the weldability of the material, the yield and tensile strength are gradually approaching to the bulk material, and the fracture status of the joint is basically ductile. The use of these metrics to evaluate the performance of joints has gradually become meaningless. However, joints are still the weak link of the piping system. It is crucial to improve the resistance to defects of joints to maintain the structural reliability of the entire piping system.

When evaluating the mechanical properties of welded joints, welding factors are generally used to describe them. One welding factor is the ratio on tensile strength or yield strength (EN 12184-2), i.e. $f_s = \frac{\bar{\sigma}_w}{\bar{\sigma}_r}$, where $\bar{\sigma}_w$ is the arithmetic mean of the tensile strength or yield strength of the weld specimens, $\bar{\sigma}_r$ is the arithmetic mean of the tensile strength or yield strength of the non-weld specimens. The other welding factor is the ratio on energy to break (EN 12184-7), i.e. $f_e = \frac{\bar{E}_w}{\bar{E}_r}$. Where, \bar{E}_w is the arithmetic mean of the energy to break of the welded specimens, \bar{E}_r is the arithmetic mean of the energy to break of the non-welded specimens. The welding factor is used for performance comparison in this paper based on the fracture stress (stress when the yield or fracture happens) and fracture energy (the area under force-displacement curve).

It is described by the Linear Elastic Fracture Mechanics (LEFM) that the crack will propagate once the actual stress intensity factor K at its tip exceeds the critical stress intensity factor of the material K_{IC} . $K = \sigma_N(\pi a)^{1/2} f(a/W)$, where σ_N is the nominal stress value, a is the crack length, and $f(a/W)$ is the shape correction function. Although polyethylene material is a viscoelastic material, short-term fracture character can still be analyzed by LEFM. During the proposed tests (Type I), with the tensile deformation increased, the stress intensity factor K_I is gradually increased. When K_I is greater than the critical stress intensity K_{IC} of the material, the fracture happens.

3.1.4. Material ability of fracture resistance

Polymer materials with good crack blocking ability first induce crazing when the notched tip is stressed intensively, which is the result of the extension of the tie molecules and the tearing of the amorphous region after the material lattice is stretched. After the expansion of the crazing, the tie molecules at the front end of the notch are gradually elongated, and then broken. As the result, the fracture energy barrier is

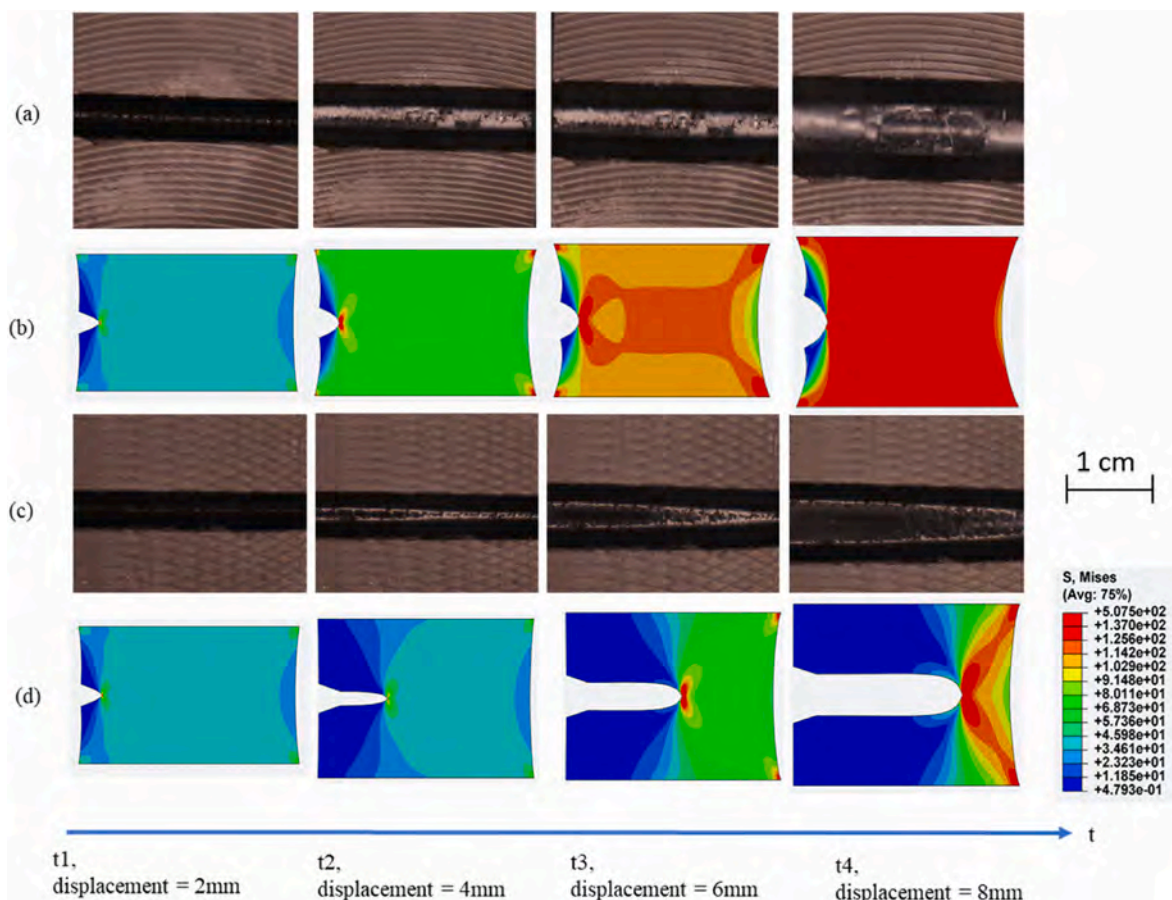


Fig. 2. The fracture process of the specimens for non-welded and welded specimens. (a) frontal view of non-welded specimen (b) lateral view of non-welded specimen (c) frontal view of welded specimen. (d) Lateral view of welded specimen.

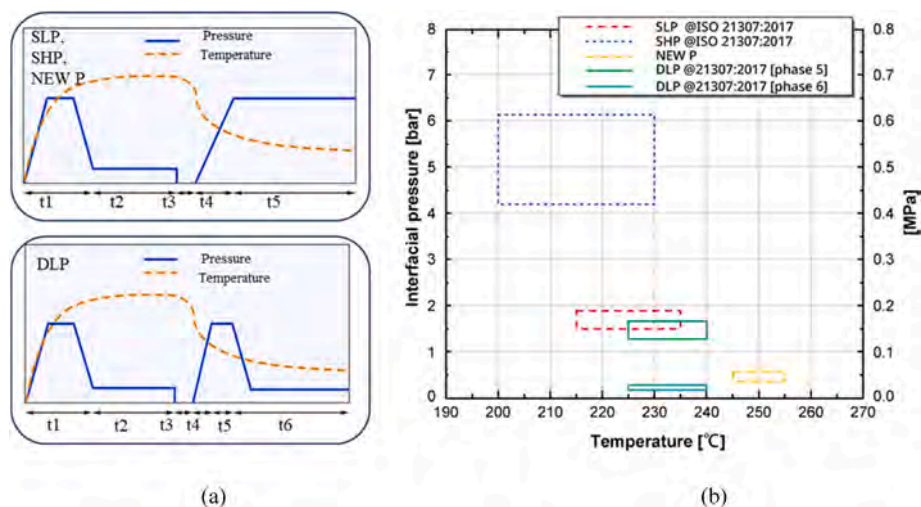


Fig. 3. Processes and values for pressure and temperatures of the studied procedures. (a) Program curves of pressure and temperature over time (b) Envelope curves of temperature and pressure.

gradually reduced, and the tie molecules at the back end are gradually sheared and fractured.

Fig. 2 presents the status of fracture at the notch area during the unilateral notched specimen test. Fig. 2(a) and (c) show the fracture process on the frontal view of the notch of a non-welded and a welded specimen respectively. Fig. 2(b) and (d) exhibit the fracture process on the lateral view of notched. ABAQUS finite element simulation is

conducted to replace the actual photos to clearly explain the stress to fracture situation. For the non-welded specimen, the width of the notch is stretched with the increase of displacement, while the notch depth changes slowly showing strong crack blocking ability. But for welded specimen, a small number of cracks are observed in the early tensile stage, then the crack propagates rapidly along the depth indicating that the molecular chain at the weld interface is pulled out, untied and

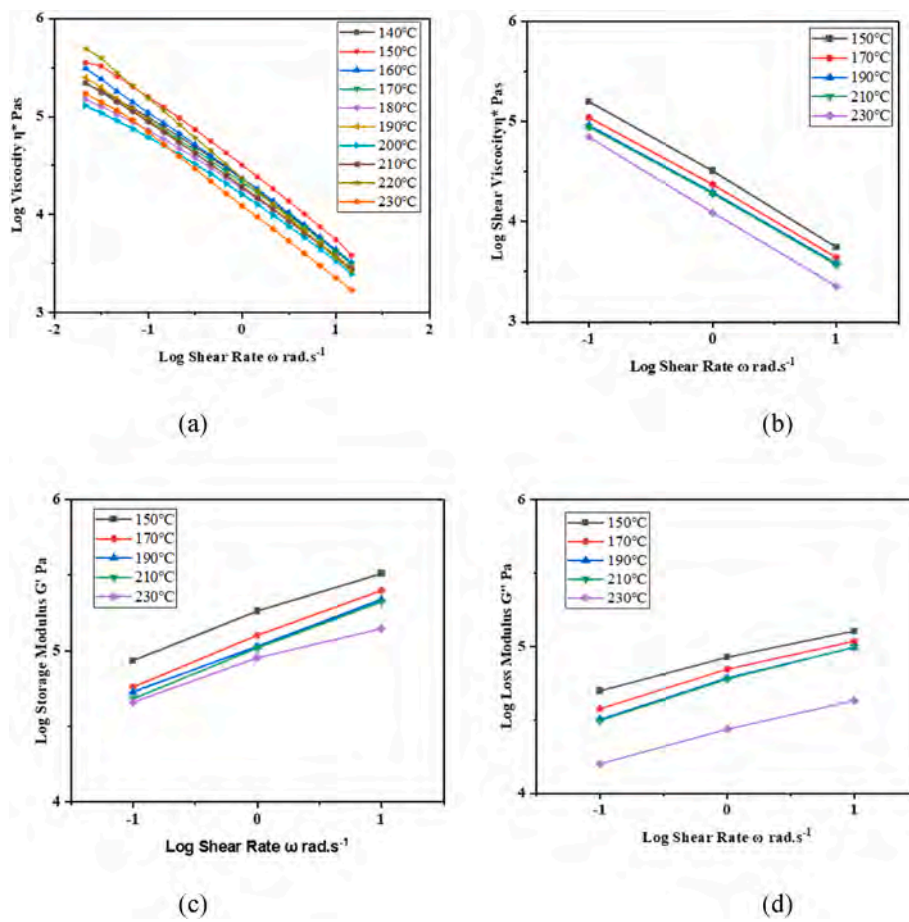


Fig. 4. RR (Rotational rheology) test for the studied material. (a) Viscosity – shear rate double-log diagrams (b) Viscosity – shear rate double-log diagrams for selected temperatures (c) Storage modulus – shear rate double-log chart for selected temperatures (d) Loss modulus – shear rate double-log chart for selected temperatures.

broken, through that the energy quickly passes through the energy barrier of the molecular chain.

Inside bimodal PE, the high-molecular-weight copolymer part participates in crystallization and becomes the “tie molecule” that runs through the crystal region. The tie of high-density molecular weight components requires large breaking energy, provides greater fracture resistance, and has high mechanical crack resistance and toughness. In the experiment, the bulk material shows superior fracture resistance, which is consistent with the molecular structure of bimodal polyethylene. The fracture behavior of the welded specimen is quite different from that of the bulk material under the condition of prefabricated V-shaped notch, which indicates that the physical properties of the material at the weld interface have changed. Obviously, the material at the welded interface does not inherit the excellent mechanical properties of the bimodal polyethylene material, and the depth and number of molecules at the welded interface may be hindered, and the strength of the molecular chain entanglement is affected. Therefore, it is necessary to improve the state of the welded interface.

3.2. Welding procedure improvement

3.2.1. Review of welding procedures

The heat and force are applied to the two faces of pipe end by the butt-fusion welding equipment. The material on the faces experiences phase changes and then cooled and forms a fusion interface by recrystallization. Fig. 3 presents the diagrams and main parameters of three procedures from ISO 21307 and the proposed new procedure. Fig. 3(a) shows the curves of pressure and temperature over time. Fig. 3(b)

demonstrates the envelope plots of the heat source temperature and interfacial pressure required. It can be seen that there is a significant difference in pressure and temperature among these procedures. The pressure and temperature range of SHP are 0.42–0.62 MPa and 200–230 °C, respectively. The pressure and temperature range of SLP are 0.15–0.19 MPa and 215–235 °C, respectively. DLP is special to other procedures as there is two pressure stages of 0.15 MPa and 0.025 MPa. The purpose of DLP maybe to reduce the joining pressure. However, the effect to interface temperature of this procedure is similar to SLP due to the similar pressure applied at the stage of 0.15 MPa, and the difference in force control logic and ability of butt-fusion equipment may cause the execution of this procedure biased. Therefore, DLP will not be discussed in this article. The authors suggest a new procedure (NEW P) for the improvement of the welding interface temperature by increasing the heat source temperature and lowering the joining pressure. The idea is similar to DLP. The diagram of pressure and temperature used is similar to that of SLP and SHP. The pressure and temperature range of NEW P is 0.04–0.06 MPa and 245–255 °C, respectively.

3.2.2. Maintain hot weld interface

Fig. 4 shows the results of RR testing. Fig. 4(a) is for the double logarithmic data obtained at different temperatures. Fig. 4(b) presents the negative correlations between viscosity and temperature or shear rate for several typical temperature points. Fig. 4(c) illustrates the negative correlations between the loss modulus and temperature or positive relations with shear rate. The storage modulus has the same character with the loss modulus, as can be seen in Fig. 4(d). Obviously, the viscosity, loss modulus and storage modulus of the studied material

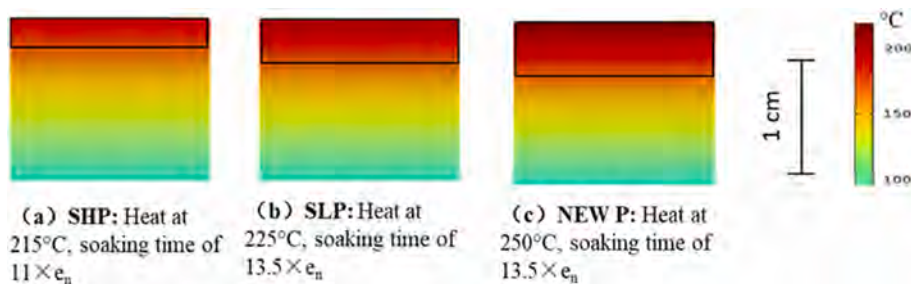


Fig. 5. Simulated diagrams of temperature distribution at the stage of heat soaking completed for one pipe end, the other end is the mirrored. Black box represents the MZ. (a) SHP (b) SLP (c) NEW P.

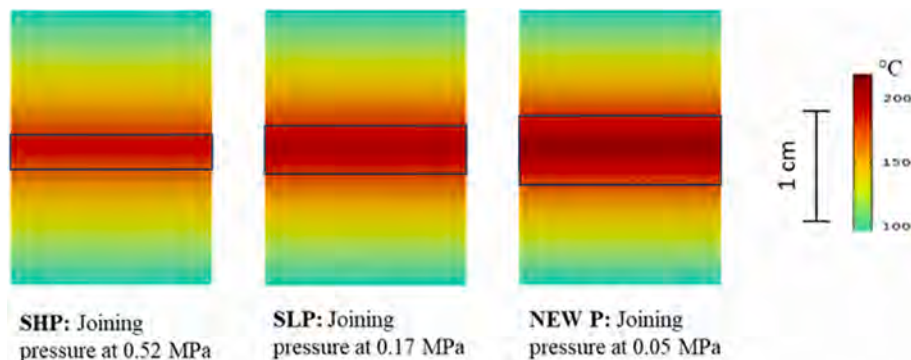


Fig. 6. Simulated diagram of temperature distribution at the stage of welding pressure established. The area inside black box represents the MZ. (a) SHP (b) SLP (c) NEW P.

all decrease with the rise of temperature when the material is in molten status.

During soaking stage of the welding process, heat is transferred along the pipe wall by heat conduction or radiation from a heat source (heating plate) and decreases in gradient along the axis. The initial temperature distribution is affected by the heat source temperature and the heat soak time. Fig. 5 shows the temperature gradient of different fusion procedures, which is simulated by COMOSL thermal software. For the sake of analysis, the influence of thermal radiation and the environment is ignored. It can be seen that the interfacial temperature and the temperature distribution width along the pipe wall of NEW P are all the highest. Comparatively, SHP is the smallest and SLP is in between.

The pressure applied to the pipe end causes the molten material flow through shearing. When the flow of molten material stops, the values of the viscosity, loss modulus, and storage modulus of the material are balanced with the applied interfacial pressure. Therefore, the values of the viscosity and modulus of the material are corresponded to its temperature. Since the temperature is distributed in a gradient along the pipe wall, the temperature of the weld interface is highest within the pipe wall. It can be seen that the greater the pressure exerted by the welding equipment, the lower temperature obtained for the weld interface, and vice versa. Fig. 6 illustrates the temperature conditions of the welding interface and its distribution when the joining pressure is established. It can be seen the NEW P acquired hottest weld interface the largest molten zone, but those two features are smallest for SHP and somewhere in between for SLP. During the welding process, the actual temperature was measured for three welding procedures by inserting three thermocouples at different locations between the two pipe ends. The positions of the sensors within weld interface are shown in Fig. 7. The highest temperature detected is the real weld interface temperature. The conclusion can be made that the temperature of the weld interface is ranking as NEW P > SLP > SHP, which validates the previous analysis.

The welding joint structure of the HDPE pipe is shown as Fig. 8(a), where BASE corresponds to the non-welded material. BEAD is the

molten material extruded outside the pipe wall. HAZ is on behalf of the zone where the heating temperature rising but not reaching the melting point or even above melting point but not deformed during joining. MZ represents the zone where the material is in molten status and been deformed during joining process. WL stands for weld interface, which is the physical interface of the connection of the two welded pipe ends with a thickness at the grade of nanometer, where chain diffusion, entanglement, and recrystallization occur. The specimens made by the three welding procedures were machined and the MZ inside the fusion joint could be observed after milling, as is shown in Fig. 8(b). For clarity, the molten zones are drawn manually, as is shown in Fig. 8(c). Measuring the width of MZ along the axial direction yields the result of NEW P > SLP > SHP, seen in Fig. 8(d), (e) and (f). The width of MZ is positively related to the heat source temperature and soaking time, and inversely proportional to the welding pressure applied during the welding process, which confirms the thermomechanical coupling analysis in the previous section.

3.2.3. Physicochemical analysis and procedure validation

As we all know, the microstructure of a material determines its mechanical properties. After the welding procedure, the material at the welding interface may have undergone a chemical change. DSC was used to test the thermal-oxygen properties of the welded interface, and the representative curves are shown in Fig. 9(a). The crystallinity of the material was calculated, as is shown in Fig. 9(b). It can be seen that there is a change in the degree of crystallinity of the material in the weld area, which are ranked as BASE > NEW P > SLP > SHP. The crystallinity test data are in good agreement with the results obtained by the proposed evaluation in later section, indicating that the fusion procedure affects the crystallinity by the welding interface temperatures. The OIT test result is presented in Fig. 9(c), and the nearly identical thermal-oxidative aging temperature of the bulk material and the welding interface of the three welding procedures are shown in Fig. 9(d). This shows none of the studied weld procedures have undergone significant

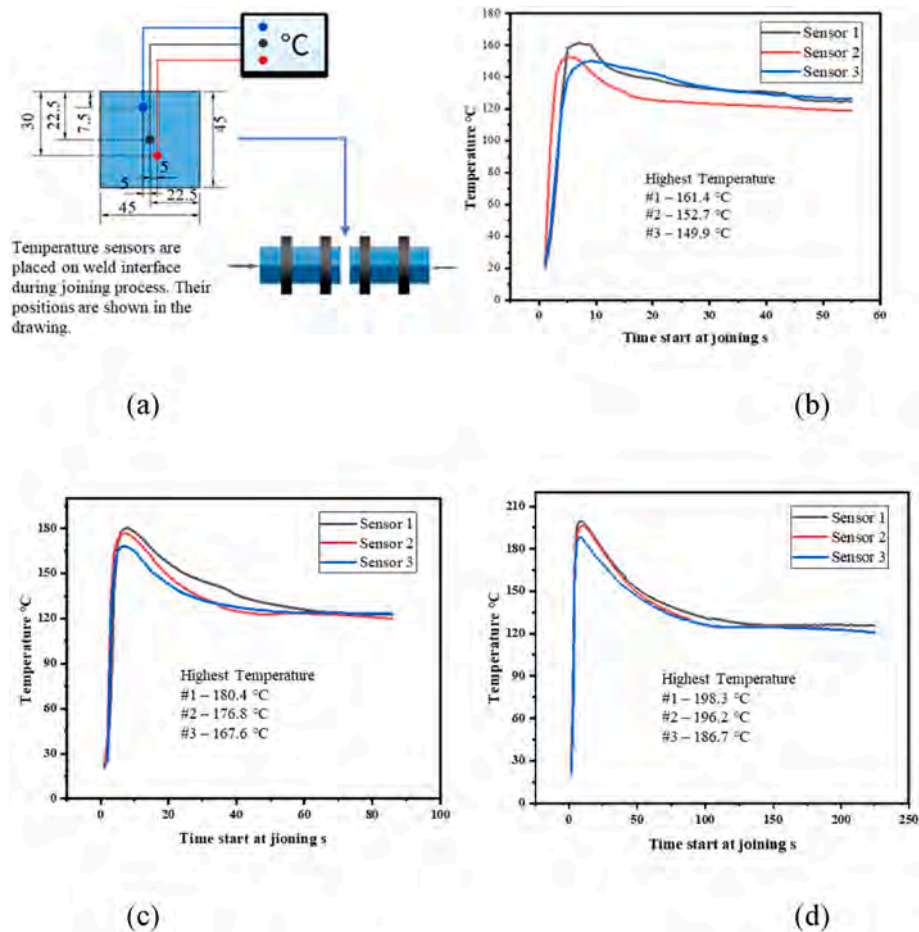


Fig. 7. Measured temperatures on the weld interface during joining process. (a) Indication of the experiment (b) SHP (b) SLP (c) NEW P.

oxidative degradation. FTIR tests shows in Fig. 9(e) that there are no new chemical groups introduced during the welding process. In summary, the proposed welding procedure is effective and feasible.

3.3. Mechanical character test with existing methods

3.3.1. Tensile strength and fracture status judgement

ISO 21307 specifies ISO 13953 as one of the welding procedure validation methods. The type B specimen is used for wall thickness beyond 25 mm and the procedure is validated if the ductile fracture happened from the tensile test. This specimen has also been used by some researchers to evaluate the performance of weld joints, as well as being used by the authors to evaluate welding procedures in the study. Fig. 10(a) shows the dimensions of the specimen and the test parameters. Fig. 10(b) is the representative force-displacement curve for each welding procedure. Through the tensile curve and fracture surface state of the tested specimens, the authors have made the conclusion that all the welding procedures had been validated as ductile fracture occurred. Fig. 10(c) shows the calculated tensile strength and the welding factor calculated from it. The order of performance is ranked as NEW P > BASE > SHP > SLP. Fig. 10(d) exhibits the obtained fracture energy and the welding factor calculated based on it. The performance can be ranked as BASE > SLP > NEW P > SHP. In the process of tensile testing, the authors observed that the yield of all specimens occurred in the middle of the axial direction. For BASE specimens, the yield strain gradually spreads to the grips and finally breaks at the arc of the specimen. For all welded specimens, the strain of middle point is continuously increased while the strain is smaller on outer sides of the specimen which are constrained by the weld beads. Then the notch formed by the angle of

weld bead and the pipe wall begins to deform, and been gradually enlarged and final teared, resulting in a rapid decrease in tensile force. As a result, the following strain is much smaller than BASE, which can be seen from Fig. 10(b). The authors believe it is not appropriate to use this specimen for the evaluation of welding performance, because the real tensile strength of the welded specimen may be amplified due to the influence of weld beads, on the contrary, the actual fracture energy may be greatly lessened. Beside, the size of weld joint areas and beads are different due to the effect of different welding procedures which may cause the extra influence on the performance evaluation.

3.3.2. Tensile impact test and fracture status judgement

Tensile impact test specified in ASTM F2634 is required by both ISO 21307 and ASTM F2620 to evaluate the short-term mechanical properties. If the state of fracture is in ductile the welding procedure is acceptable. The use of rapid tensile impact testing can reflect the behavior of a material when it is subjected to drastically varied external forces, such as seismic waves. Authors have used this method to test the performance of BASE, SHP, and SLP. Fig. 11(a) shows the shape and size of the specimen, as well as the test parameters. Fig. 11(b), (c) and (d) are the force-displacement curves of the BASE, SHP, and SLP acquired during the test respectively. According to the test results, all the specimens showed ductile fracture, and the average impact stress obtained are basically the same. However, for SHP specimens, the force-displacement curves are very discrete of each test. Also, it was observed that the fracture points of the welded specimens are discrete, some fracture at bead notches and some fracture on the bulk material. This may be due to the narrow melting zone MZ of SHP, as well as the presence of the weld bead. Therefore, the authors believe this method is

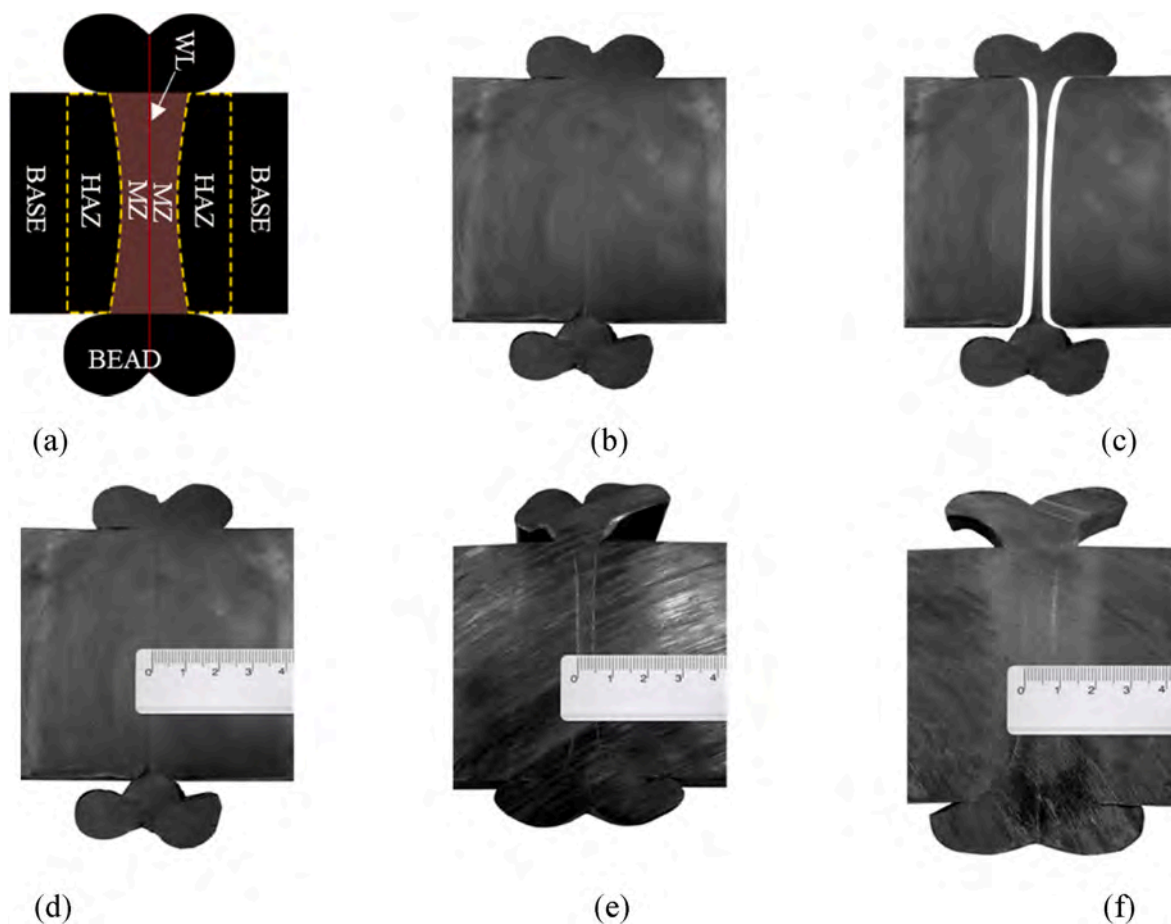


Fig. 8. The observation of MZ inside the welding joints for different welding procedures. (a) Diagram of different zones existed at the welding joint (b) Actual profile of the welded joint (c) Manual separation drawing about MZ (d) MZ width of SHP (e) MZ width of SLP (f) MZ width of NEW P.

not appropriate to be used for welding procedures performance evaluation. Which is consistent with the opinion from some literatures which have been described in the introduction section.

3.3.3. Fracture energy test with waisted specimens

As can be seen in the introduction section, tensile testing using waisted specimens is a widely accepted method for evaluating the performance of welded joints. The waisted specimen is used in this study too. Fig. 12 (a) presents the dimensions of the specimen and test parameters. Fig. 12 (b) is the representative force-displacement curves extracted from the testing. When using tensile strength to calculate the welding factor, it is found that the result is as $SLP > BASE > SHP = NEW P$, as is seen in Fig. 12(c). When the fracture energy is used for the assessment, the result is ranked as $BASE > NEW P > SLP > SHP$, as is seen in Fig. 12(d). Since the weld joint uses a circular arc with a radius of 5 mm for stress concentration, it can ensure the fracture occur at the joint. This kind of specimen is good to distinguish the properties between the welded material and the non-welded material. However, when the arc is used to concentrate the stress on the weld interface, the weld interface is still affected by the material properties of the surrounding molten zone or heat-affected zone. While, different shapes and widths of the molten zone (MZ) and heat-affected zone (HAZ) are created by different welding procedures. Therefore, the weld interface properties from different procedures cannot be accurately characterized. This has been confirmed by the difference between tensile strength and fracture energy.

3.4. Tests of the proposed evaluation method

3.4.1. Unilateral notched specimen test

Notched specimens are used in linear elastic fracture mechanics to test material fracture toughness, and is also used to test the fracture toughness of polymeric materials by researchers, as is mentioned in the introduction section. In view of this, a unilateral notched specimen is designed by the authors and is applied for quasi-static axial tensile test to evaluate the fracture resistance of the welded interface material to defects. The specimen designed is able to concentrate the stress through the weld interface by locate the notch tip at the weld interface, so that the fracture can occur at the welded interface during tensile. The specific dimensions and test parameters of the specimen used are shown in Fig. 13(a). The force-displacement curves acquired during the test is given in Fig. 13(b). The data in Fig. 13(c) compares the short-term mechanical properties of several welding procedures, and the welding factors are calculated on the maximum fracture stress. It can be seen that the welding factors is ranked as $BASE > NEW P > SLP > SHP$. Among them, SHP is 11.3 % lower than BASE, and SLP is 4.9 % lower than BASE. NEW P is 10.9 % higher than SHP and 4.5 % higher than SLP. The data in Fig. 13(d) represents the energy consumed during the fracture process that is used to calculate the welding factors to compare those welding procedures. It can be seen that $BASE > NEW P > SLP > SHP$, which is consistent with the comparison of the maximum fracture stress. The conclusion is also made that the performance gap of the welding factor is increased by using energy calculation, in which SHP is 73.5 % lower than BASE, and SLP is 53.8 % lower than BASE, while NEW P is 50.7 % higher than SHP and 31 % higher than SLP. This evaluation method is able to distinguish the mechanical properties of different welding

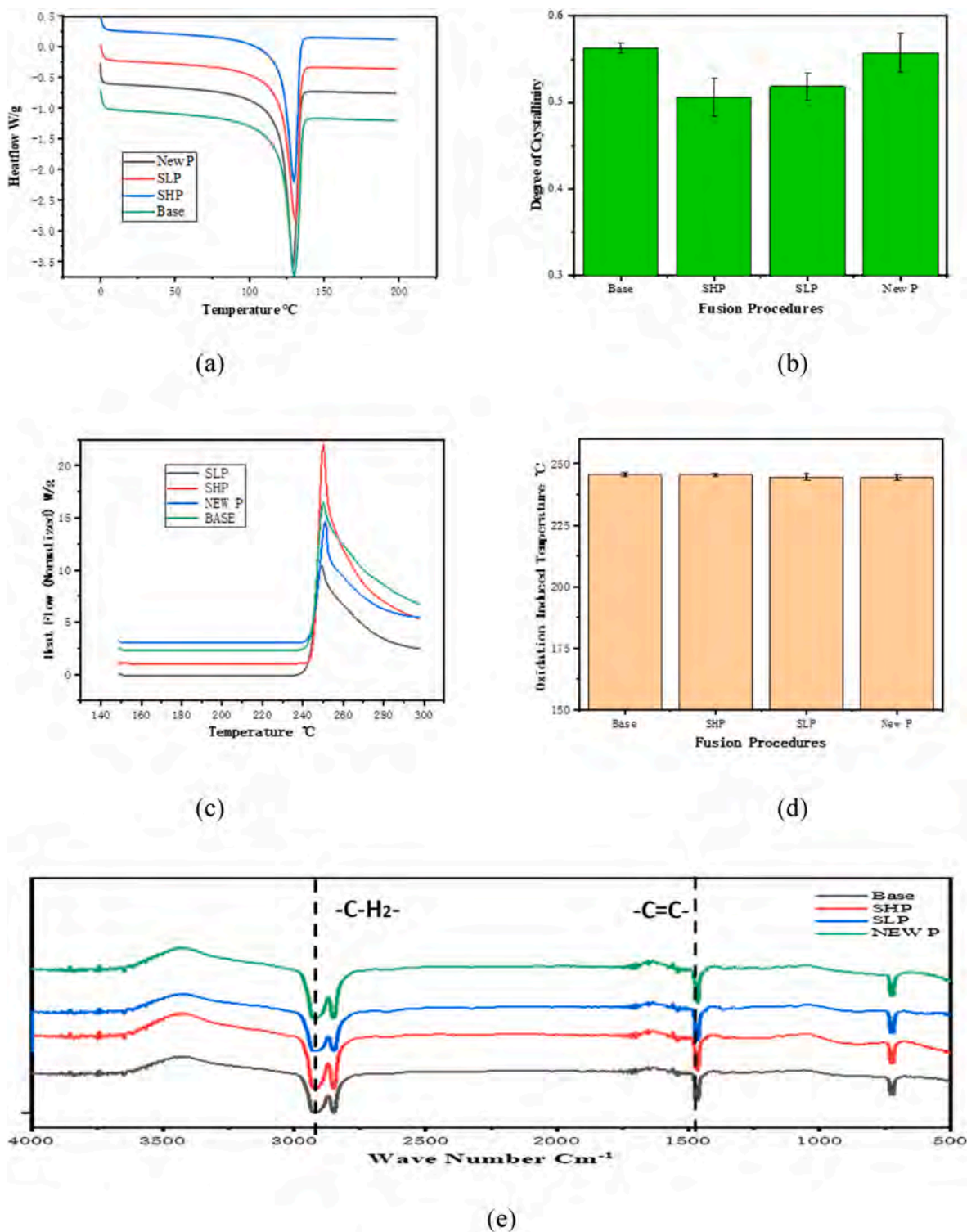


Fig. 9. The physicochemical property analysis. (a) Representative diagram from DSC test (b) Crystallinity calculated from DSC test (c) Representative diagram from OIT test (d) Oxidation induced temperature calculated from OIT test (e) Representative diagram from FTIR test.

programs, and show that the recommended welding procedure has the best performance.

3.4.2. Weld interface crack specimen test

The current research on the welding performance of polyethylene pipes is to study the entire joint area as a whole. However, as can be seen from Fig. 8(a), there are different zones at the weld joint. The material properties at the welded joint may differ in MZ, HAZ and WL. The

centerline of the V-notch of the specimen used in this paper is approximately passing through the fusion interface WL, but there may still be deviations during sampling. Therefore, a thin circular iron sheet is placed on the pipe end during joining process to further make a crack on the welding interface. Which is also used to simulate the welding defects may occur. Detailed dimensions and test parameters are specified in Fig. 14(a). Fig. 14(b) is the representative force-displacement curves acquired during the test. The data in Fig. 14(c) compares the short-term

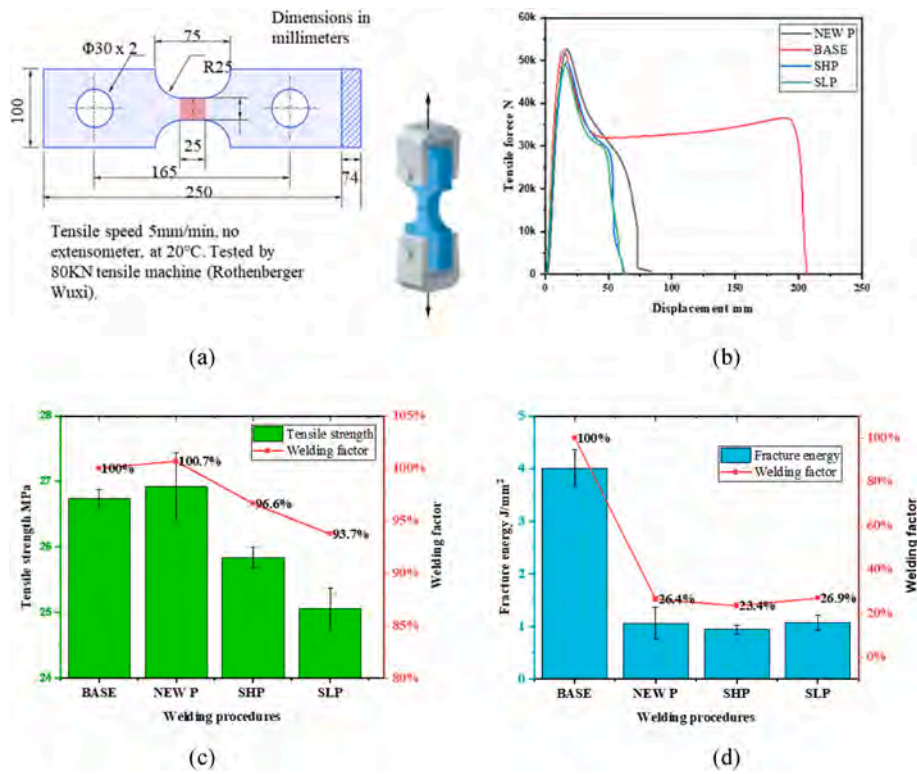


Fig. 10. Tensile test with the method of ISO 13953 and type B specimen. (a) Specimen dimensions (full wall thickness) and test parameters (b) Representative force-displacement curve of each produced (c) Tensile strength and welding factors (d) Fracture energy and welding factors.

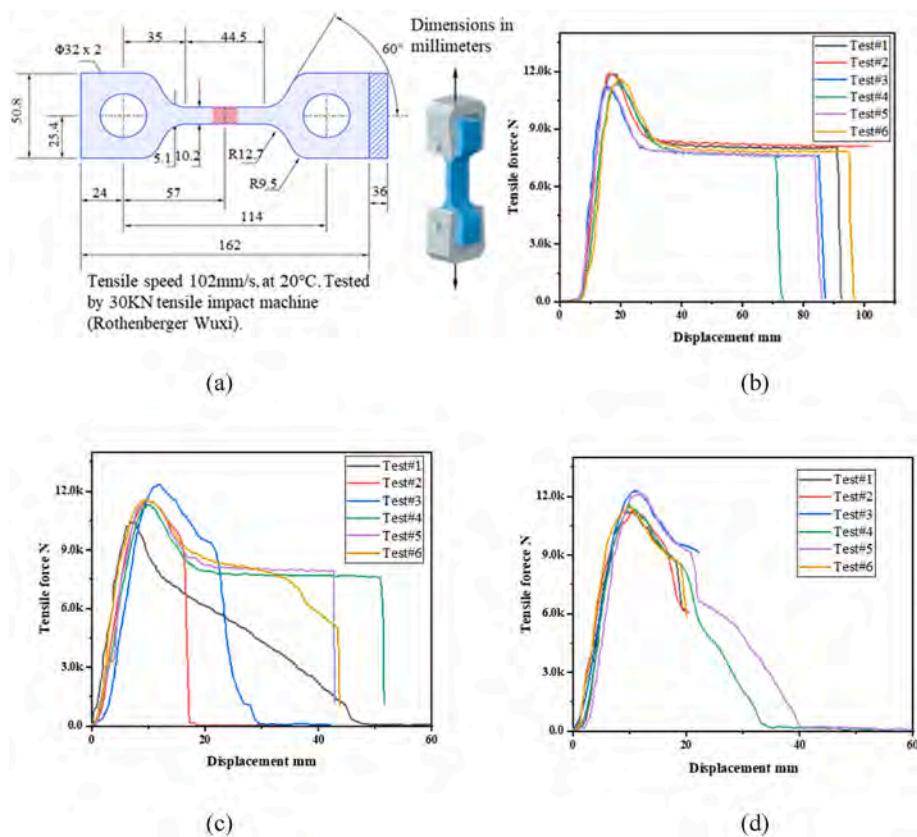


Fig. 11. Tensile impact test by the method of ASTM F2634. (a) Dimension of specimens and test parameters (b) Force-displacement of BASE (c) Force-displacement of SHP (d) Force-displacement of SLP.

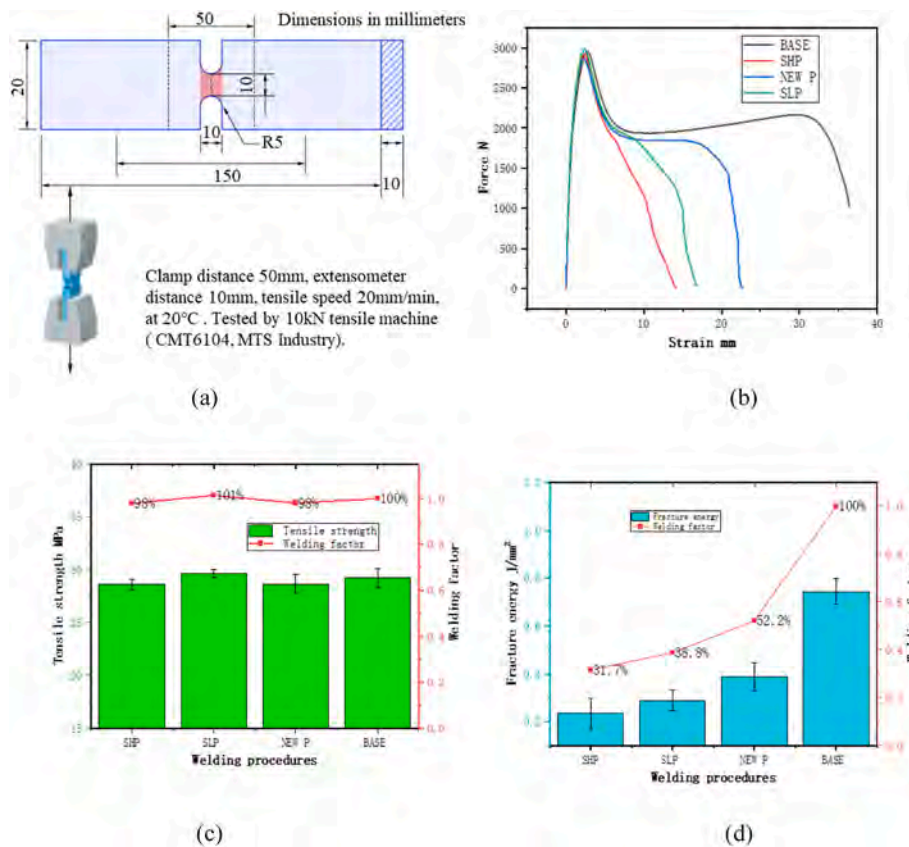


Fig. 12. Tensile test with the arc waisted specimen (a) Specimen size and test parameters (b) Representative force-displacement curves (c) Result of tensile strength and welding factors (d) Result of fracture energy and welding factors.

mechanical properties of several welding procedures using the maximum fracture stress, and welding factors are calculated accordingly. It can be seen that the performance is as the sequence of NEW P > SLP > SHP. Among them, NEW P is 39 % higher than SHP and 17 % higher than SLP. The data in Fig. 14(d) represents the energy consumed during the fracture process and is used to calculate the welding factors. It can be seen that NEW P > SLP > SHP, in which NEW P is 225 % higher than SHP and 116 % higher than SLP. Obviously, all values are still ranked as NEW P > SLP > SHP. This result is consistent with that for the V-notch specimen testing. It approves that the mechanical properties of the weld interface can be analyzed by using tensile test with the specimens having unilateral V-shaped notched or surface crack across the welding interface. But the performance gap among three welding procedures is further enlarged by using interface crack with both fracture stress and energy. Which may also indicate that the defects from welding process maybe more danger to the pipe system.

3.4.3. Fracture status and morphology study

Photographs of the fracture surfaces of the test specimens are taken from the unilateral notched specimens (chapter 3.4.1), shown in Fig. 15. It can be seen that the fracture surface morphology is quite different among bulk material and welding procedures. The BASE shows typical characteristics of ductile with strong toughness. The ligament is largely stretched before break then sheared during fracture process. The fracture surface of NEW P shows longer bulges first and then sheared. The fracture surface of SHP exhibits small bulges at beginning and then large bulges afterwards, which shows the ligament is not stretched long enough during fracture. The elongation of ligament of the SLP specimen is between SHP and NEW P. The morphology differences indicate that the ductility performance can be ranked as BASE > NEW P > SLP > SHP, which are in good agreement with the data from the tensile test.

In order to avoid the influence of uneven stress and tensile strain rate

of unilateral notched specimens on the observation of the fracture morphology, the circular notched round bar specimens are used and subjected for fast and slow tensile tests. The specific dimensions of the specimen and test parameters are shown in Fig. 16(a). Fig. 16(b) and (c) are the force-displacement curves acquired for test speed of 50 mm/min and 0.5 mm/min respectively. Fig. 16(d) exhibits all the normal photos and microscope cloud images taken for all the fractured surface. It can be seen that the bulges of BASE are much higher both at the tensile rates of 50 mm/min and 0.5 mm/min, and the NEW P is very close to it. The SHP has the least bulges at both 50 mm/min and 0.5 mm/min, basically suggesting the brittle rupture state at a tensile rate of 50 mm/min. The bulges of SLP are longer than SHP at both tensile rates, but still shorter than BASE and NEW P. The displacement curves are also in good relations with the fracture surface morphologies. The cross-sectional morphological characteristics of these specimens can also confirm the rationality of the new proposed evaluation method.

3.4.4. Test method validation analysis

At present, the tensile strength test of fusion joints is basically empirical, and it is difficult to use the test data for the reliability design and calculation of pipeline structures. The thin waist fracture energy test is actually a type of defect fracture test, but it is difficult to correlate the test results with the allowable defects. The unilateral notched specimens recommended by the authors mimic the stress concentrations caused by external forces such as sharp stones, or pipe misalignment and welding bead. Weld interface crack specimens can simulate the defects existed on the weld interface, such as the coating peeling from the hot plate. Other defects introduced during the welding process, such as cold welding, over heat, as well as water, oil stains, soil, etc. may cause incomplete fusion, material degradation, bubbles, inclusions, etc. which may cause the similar failures as the weld interface crack. It enables the experimental data to be correlated to the types and sizes of defects allowed in

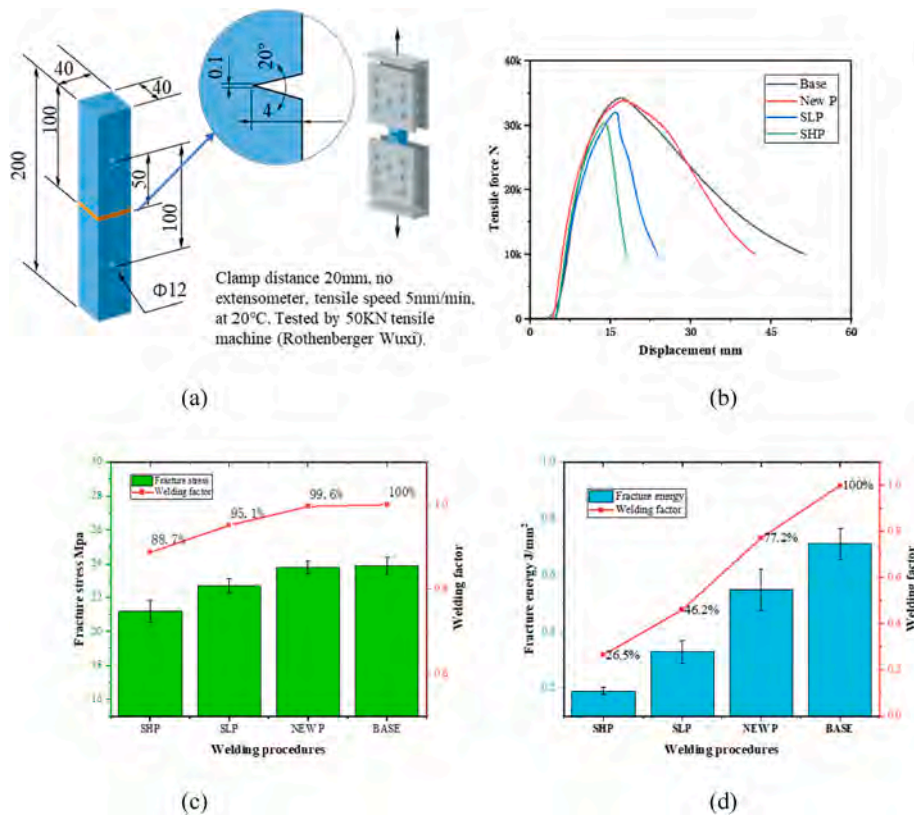


Fig. 13. Tensile test with the unilateral notched specimens (a) Specimen size and test parameters (b) Representative force-displacement curves (c) Result of fracture stress and welding factors (d) Result of fracture energy and welding factors.

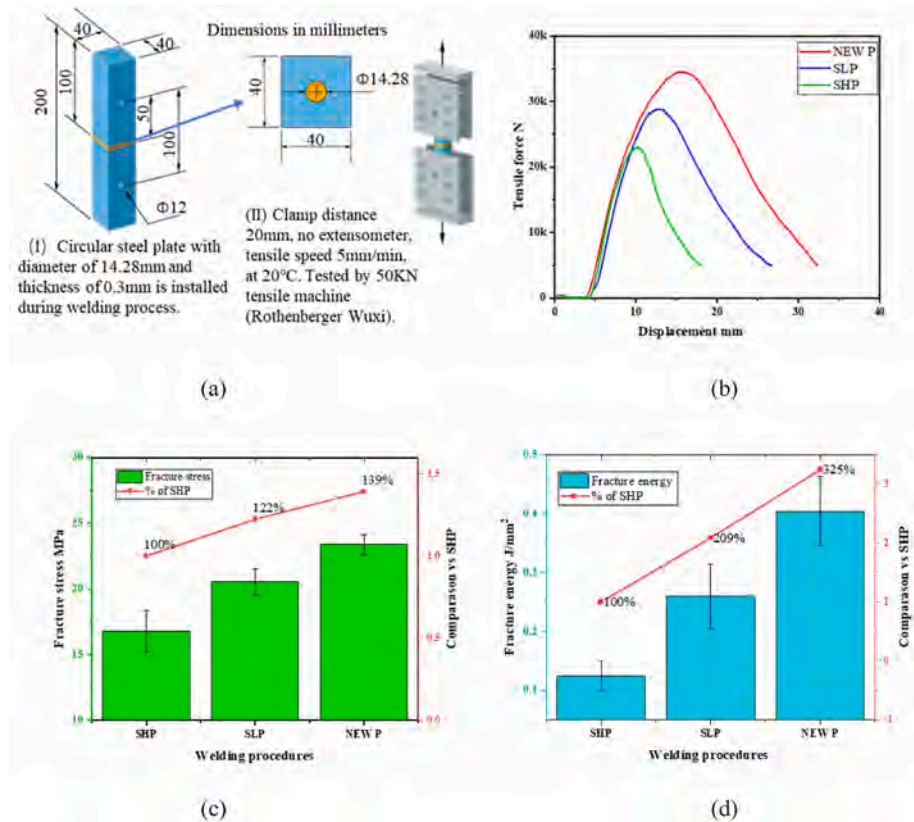


Fig. 14. Tensile test with weld interface crack specimens (a) Specimen size and test parameters (b) Representative force-displacement curves (c) Result of fracture stress and welding factors (d) Result of fracture energy and welding factors.

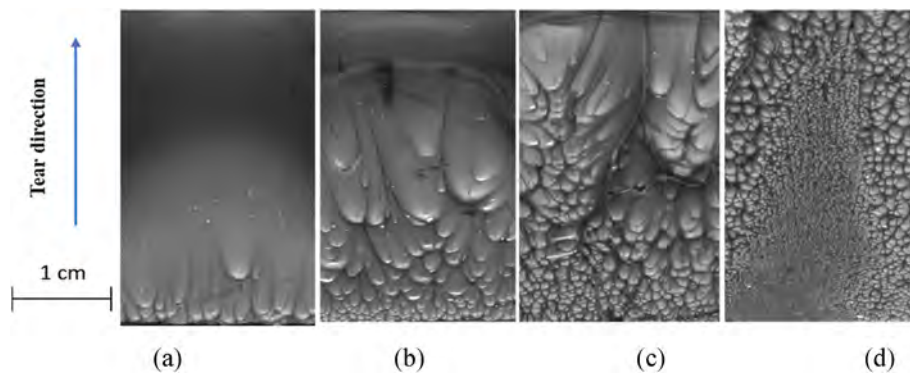


Fig. 15. The fracture morphology of unilateral notched specimen tests. (a) BASE (b) NEW P (c) SLP (d) SHP.

the design of the piping system by means of stress intensity factors, maximum failure stresses or energies.

For the unilateral notched test, we have performed two additional sets of experiments on BASE and SHP materials. The specimens of group 1 have the same shape and size, but different notch ratio. The specimens of group 2 have the same shape and notch ratio, but different sizes. The specific specimen dimensions and test parameters are shown in Fig. 17 (a). Fig. 17(b) and (c) are the values of fracture energy and fracture stress of BASE and SHP specimens from the group 1 respectively. It can be seen that the fracture energy and fracture stress values of the welding material are lower than those of the bulk material. With the increase of the notch ratio of the specimens, the fracture energy of the specimens shows a downward trend, but the fracture stress basically remains the same. Fig. 17(d) and (e) show the fracture energy and stress values of BASE and SHP specimens of the group 2 respectively. It can be seen that the fracture energy and stress values of the welding material are much lower than those of the bulk material, and with the increase of the overall size (cross-sectional area) of the specimens, their fracture stress shows a downward trend while the trend of fracture energy is reversed.

Together with the test results shown in the previous sections, it can be seen that the material properties of the weld interface have changed significantly compared to the bulk material. Based on the viscoelastic characteristics of HDPE, the fracture resistance to defect will also be nonlinear, that is, the critical stress intensity factor (K_{IC}) of type I defects is nonlinear for the polyethylene weld interface. Correlating the fracture stress, fracture energy, and stress intensity factor shall also take into account the shape of the defects and their location and size in the material. In order to establish a more accurate relationship between material defect failure and provide a theoretical basis for practical application, it is also necessary to consider the test rate, temperature, time and other factors. When analyzing the welding performance of thick-walled polyethylene pipes, it is necessary to use large-size specimens for analysis. In authors' opinion, the cross-section of the specimen should be at least the values of full wall thickness in two dimensions, and specimens should be subjected to the tests of notched and interface cracks from multiple defect dimensions to gain a more comprehensive understanding of the impact of welding procedures and defect conditions on the mechanical properties of piping systems.

4. Conclusions

In this study, the authors have used several well-established test methods and the proposed method to evaluate the mechanical properties of welded joints of thick-walled pipes under different fusion procedures. An improved butt fusion welding procedure has been proposed and experimentally verified. The welded interface properties of thick-walled polyethylene pipes are affected by the thermal-mechanical coupling status, and the mechanical properties can be varied by changing the welding parameters. The defect-based specimens can

imitate the actual defect state, which not only can distinguish the influence of different welding procedures, but also quantitatively establish the design basis for the allowable of welded defects in pipeline application process.

1. The improved performance of fracture resistance from the proposed welding procedure in comparison to SHP and SLP can be verified by the proposed evaluation method.
2. Higher welding interface temperature and the width of the melting zone can be obtained by increasing the temperature of the heat source, prolonging the soaking time and reducing the welding force.
3. The interfacial temperature and the width of the melt zone contribute to the ability of the welding interface to resist the failure of notches or cracks.
4. The shape of unilateral notch specimen and weld interface crack specimen can ensure the fracture occur at the weld interface, so that the fracture resistance of the weld interface can be evaluated.
5. The influence of specimen shape and size on the test results should be considered when analyze the welding performance of large-diameter thick-walled pipes.
6. Multi-dimensional testing of notched or cracked specimens can provide accurate data to establish quantitative metrics on the design matrix of defects in the piping system.

In order to accurately reflect the performance of weld joints, the tests performed in this paper are still insufficient, such as the test of larger specimens, and the long-term performance test based on the time dimension. The authors expect more research data and analytical methods reported to enrich the dimensions of understanding and application optimization of welding process of HDPE pipes.

CRedit authorship contribution statement

Zhenchao Wang: Writing – review & editing, Writing – original draft, Validation, Supervision, Resources, Project administration, Methodology, Investigation, Formal analysis, Data curation, Conceptualization. **Shijun Zhang:** Visualization, Investigation, Data curation. **Jichun Qie:** Visualization, Methodology, Investigation, Data curation. **Qijiang You:** Validation, Software, Investigation, Data curation. **Lu Xu:** Visualization, Investigation, Formal analysis, Data curation. **Qiuju Zhang:** Writing – review & editing, Validation, Supervision, Resources, Project administration, Methodology, Investigation, Conceptualization.

Declaration of competing interest

The authors declare that they have no known competing financial interests or personal relationships that could have appeared to influence the work reported in this paper.

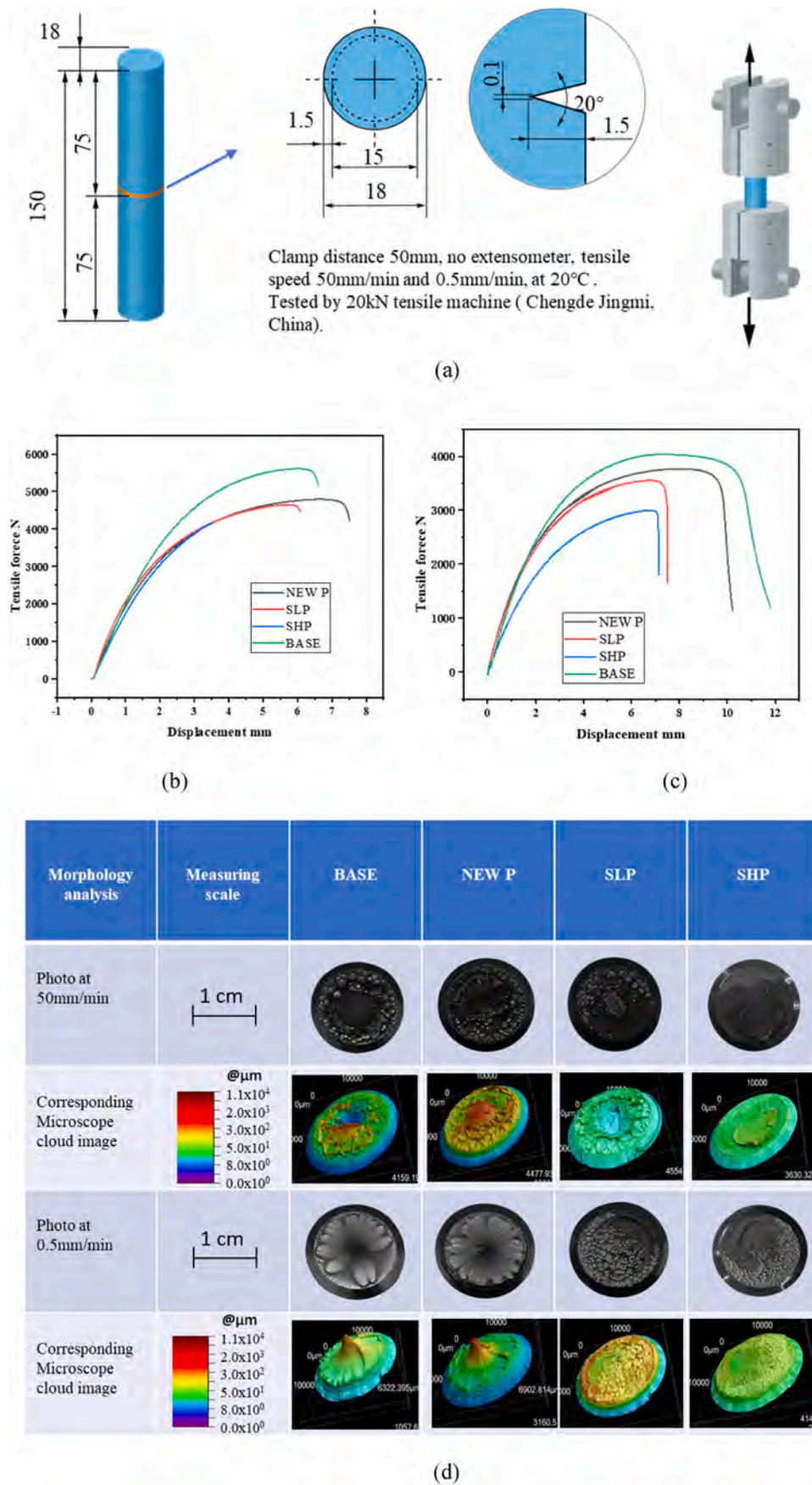


Fig. 16. Morphological analysis for circular notched round bar specimens. (a) Specimen size and test parameters (b) Force-displacement curves at 50 mm/min (c) Force-displacement curves at 0.5 mm/min (d) Photos of all fracture surface.

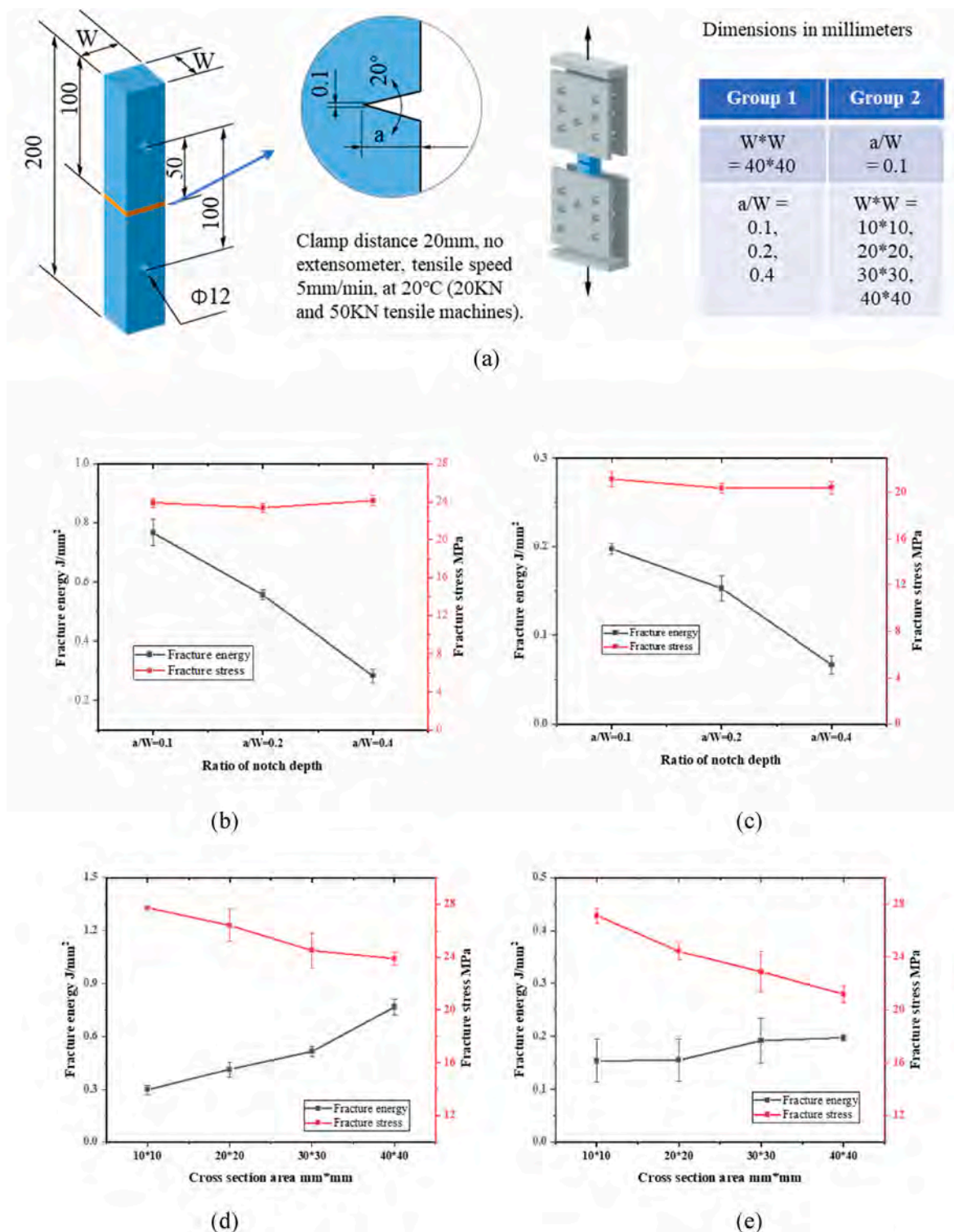


Fig. 17. Tensile test for different specimens size or notch ratio (a) Specimens and test parameters (b) Fracture energy and stress of BASE from group 1 (c) Fracture energy and stress of SHP from group 1 (d) Fracture energy and stress of BASE from group 2 (e) Fracture energy and stress of SHP from group 2.

Data availability

Data will be made available on request.

References

[1] Chen Zou, Quan Wang, Guifu Si, et al., A co-anchoring strategy for the synthesis of polar bimodal polyethylene, Nat. Commun. 14 (2023) 1442.

[2] Y.X. Zhang, X.H. Kang, Z.B. Jian, Selective branch formation in ethylene polymerization to access precise ethylene-propylene copolymers, Nat. Commun. 13 (2022) 725.

[3] F.P. Alt, L.L. Bohm, H.F. Enderle, J. Berthold, Bimodal Polyethylene-Interplay of catalyst and process, Macromol. Symp. 163 (2001) 135-143.

[4] Cheol Jeong, Francis W. Starr, Kathryn L. Beers, et al., Influence of functionalization on the crystallinity and basic thermodynamic properties of polyethylene, Macromolecules 56 (2023) 3873-3883.

[5] Fabian Friedrich, Michael Gehde, Heated tool welding of thick-walled parts, AIP Conf. Proc. 2289 (2020) 050021.

- [6] S. Kalyanam, P. Krishnaswamy, Y. Hioe, et al., A fracture mechanics approach to service life prediction of HDPE fusion joints in nuclear applications, *Plast. Eng.* (2015).
- [7] N-755-4 ASME BPVC.CC.NC-2021, Use of Polyethylene (PE) Class 3 Plastic Pipe Section III, Division 1, CODE CASES Nuclear Components.
- [8] Hongbin Dai, Jun Peng, The Effects of Welded Joint Characteristics on its Properties in HDPE Thermal Fusion Welding [J], World Scientific, 2017.
- [9] Jong-Sung Kim, Young-Jin Oh, Sun-Woong Choi, et al., Investigation on the thermal butt fusion performance of buried high density polyethylene piping in nuclear power plant, *Nucl. Eng. Technol.* 51 (2019) 1142–1153.
- [10] Subin Damodaran, Tobias Schuster, Karsten Rode, et al., Measuring the orientation of chains in polypropylene welds by infrared microscopy: a tool to understand the impact of thermo-mechanical treatment and processing, *Polymer* 60 (2015) 125–136.
- [11] Xinyu Nie, Dongsheng Hou, Jinyang Zheng, et al., Eigen-line in welded structures of thermoplastic polymers, *Polym. Test.* 57 (2017) 209–218.
- [12] Min Kwan Kang, Sunwoong Choi, Hyun Hoon Song, Microstructural investigation of butt-fusion joint in high-density polyethylene pipes using wide- and small-angle X-ray scattering, *Applied Polymer Science* (2018).
- [13] Shijun Wang, Jiaxin Shi, Takayuki Shimizu, et al., Two step heat fusion kinetics and mechanical performance of thermoplastic interfaces, *Scientific Reports* 12 (2022) 5701.
- [14] Feifei Yan, Hanchuan Li, Shanlin Cui, et al., Effects of combined melt stretching and fast cooling fields on crystallization of high-density polyethylene, *Polymer* 275 (2023) 125930.
- [15] Ting Ge, Gary S. Grest, Mark O. Robbins, Tensile fracture of welded polymer interfaces: miscibility, entanglements, and crazing, *Macromolecules* 47 (2014) 6982–6989.
- [16] Fotis Christakopoulos, Enrico Troisi, Nic Friederichs, et al., “Tying the knot”: enhanced recycling through ultrafast entangling across ultrahigh molecular weight polyethylene interfaces, *Macromolecules* 54 (2021) 9452–9460.
- [17] Huan Sheng Lai, Nwe Ni Tun, Kee Bong Yoon, et al., Effects of defects on failure of butt fusion welded polyethylene pipe, *Int. J. Pres. Ves. Pip.* 139–140 (2016), 1174–122.
- [18] J. Mikula, P. Hutař, E. Nezbedová, et al., On crack propagation in the welded polyolefin pipes with and without presence of weld beads, *Mater. Des.* 87 (2015) 95–104.
- [19] Yu Sun, Yun-Fei Jia, Muhammad Haroon, et al., Welding residual stress in HDPE pipes: measurement and numerical simulation, *J. Pressure Vessel Technol.* (2018).
- [20] DVS 2207-1, Welding of Thermoplastics -Heated Element Welding of Pipes, Piping Parts and Panels Made Out of Polyethylene, 2015.
- [21] Tarek M.A. A. El-Bagory, Hossam E.M. Sallam, Maher Y.A. Younan, Evaluation of fracture toughness behavior of polyethylene pipe materials, *J. Pressure Vessel Technol.* 137 (DECEMBER 2015) 061402, <https://doi.org/10.1115/1.4029925>.
- [22] Tarek M.A. A. El-Bagory, Hossam E.M. Sallam, Maher Y.A. Younan, Validation of linear elastic fracture mechanics in predicting the fracture toughness of polyethylene pipe materials [C], in: *Proceedings of the ASME 2015 Pressure Vessels and Piping Conference PVP2015, PVP2015-45651*, 2015. Boston, Massachusetts, USA.
- [23] T. El-Bagory, Maher Y.A. Younan, Hossam E.M. Sallam, Lotfi A. Abdel-Latif, Limit load determination and material characterization of cracked polyethylene miter pipe bends, *J. Pressure Vessel Technol.* 136 (2014), <https://doi.org/10.1115/1.4026330>, 041203-1.
- [24] Anatoliy Galchun, Nikolay Korab, Volodymyr Kondratenko, et al., Nanostructurization and thermal properties of polyethylene welds, *Nanoscale Res. Lett.* 10 (2015) 138.
- [25] GIS/PL2-3:2015, Polyethylene Pipes and Fittings for Natural Gas and Suitable Manufactured Gas Part 3: Butt Fusion Machines and Ancillary Equipment.
- [26] WIS 4-32-8, SPECIFICATION FOR THE FUSION JOINTING OF POLYETHYLENE PRESSURE PIPELINE SYSTEMS USING PE80 AND PE100 MATERIALS.
- [27] GB/T 32434-2015, Plastics Pipes and Fittings-Butt Fusion Jointing Procedures for polyethylene(PE) Pipes and Fittings Used in the Construction of Gas and Water Distribution Systems.
- [28] ASTM F2620-20, Standard Practice for Heat Fusion Joining of Polyethylene Pipe and Fittings.
- [29] ISO 21307:2017 [E], Plastics Pipes and Fittings – Butt Fusion Jointing Procedures for Polyethylene (PE) Piping Systems.
- [30] ASTM F2634-15, Standard Test Method for Laboratory Testing of Polyethylene (PE) Butt Fusion Joints Using Tensile - Impact Method.
- [31] DVS 2203-2 2010, Testing of Welded Joints between Panels and Pipes Made of Thermoplastics -Tensile Test.
- [32] DVS 2203-5 1999, Testing of Welded Joints of Thermoplastics Plates and Tubes: Technological Bend Test.
- [33] DVS 2203-1 2003, Testing of Welded Joints of Thermoplastic Sheets and Pipes Test Methods -Requirements.
- [34] ISO 13953:2001(E), Polyethylene (PE) Pipes and Fittings-Determination of the Tensile Strength and Failure Mode of Test Pieces from a Butt-Fused Joint.
- [35] BS EN12814-1:2000, Testing of Welded Joints of Thermoplastics Semi-finished Products-Part 1: Bend Tests.
- [36] EN 12814-2:2021 E, Testing of Welded Joints of Thermoplastics Semi-finished Products-Part 2: Tensile Test.
- [37] BS EN 12814-7:2002, Testing of Welded Joints of Thermoplastics Semi-finished Products-Part 7: Tensile Test with Waisted Test Specimens.
- [38] Sunwoo Kim, Taemin Eom, Wonjae Lee, et al. Tapered Waist Tensile Specimens for Evaluating Butt Fusion Joints of Polyethylene Pipes—Part 1: Development [J].
- [39] Tao Liao, Xintong Zhao, Phil Coates, et al., Structural heterogeneity dependence of the fracture feature distribution in the tensile elongation of microinjection molded polyethylene, *Macromolecules* 56 (2023) 1983–1994.
- [40] Mohommad Shapheek, Naveen Shrivastava, Optimization of cooling time for polyethylene fusion joints, *Mater. Today: Proc.* 28 (2020) 1267–1272.
- [41] Tarek M.A.A. El-Bagory, Hossam E.M. Sallam, Maher Y.A. Younan, Effect of strain rate, thickness, welding on the J–R curve for polyethylene pipe materials, *Theor. Appl. Fract. Mech.* 74 (2014) 164–180.
- [42] Mike Troughton, Amir Khamsehzhad, SHORT-TERM and long-term mechanical testing to evaluate the effect of flaws in butt FUSION joints in polyethylene pipes [C], in: *Proceedings of the ASME 2016 Pressure Vessels and Piping Conference PVP2016, July 17-21, 2016, Vancouver, British Columbia, Canada.*
- [43] Muhammad Shaheer, Effects of Welding Parameters on the Integrity and Structure of HDPE Pipe Butt Fusion Welds [D], Brunel University, London, 2017.
- [44] S. Kim, T. Eom, W. Lee, S. Choi, Tapered waist tensile specimens for evaluating butt fusion joints of polyethylene pipes—Part 1: development, *Polymers* 14 (2022) 1187, <https://doi.org/10.3390/polym14061187>.
- [45] Tarek M.A. A. El-Bagory, Hossam E.M. Sallam, Maher Y.A. Younan, Effect of loading rate and pipe wall thickness on the strength and toughness of welded and unwelded polyethylene pipes, *J. Pressure Vessel Technol.* (2021) 011505, <https://doi.org/10.1115/1.4047444>, 143.
- [46] Pyeong An Lee, Sunwoo Kim, Bob Stakenborghs, et al., Development of hydro-axial tension method for whole pipe butt-fusion joint tensile test, *Polym. Test.* 109 (2022) 107553.
- [47] Jianfeng Shi, Ying Feng, Yangji Tao, et al., Evaluation of the seismic performance of butt-fusion joint in large diameter polyethylene pipelines by full-scale shaking table test, *Nucl. Eng. Technol.* 55 (2023) 3342–3351.
- [48] Shushan Chen, Huan Sheng Lai, Rong Lin, et al., Study on the creep properties of butt fusion-welded joints of HDPE pipes using the nanoindentation test, *Weld. World* 66 (2022) 135–144.
- [49] ISO12176-1, Plastics Pipes and Fittings - Equipment for Fusion Jointing Polyethylene Systems - Part 1: Butt Fusion, 2017.
- [50] Jung-Wook Wee, Ilhyun Kim, Min-Seok Choi, et al., Characterization and modeling of slow crack growth behaviors of defective high-density polyethylene pipes using stiff-constant K specimen, *Polym. Test.* 86 (2020) 106499, <https://doi.org/10.1016/j.polymertesting.2020.106499>.
- [51] Suleyman Devenci, Nisha Antony, Birkan Eryigit, Effect of carbon black distribution on the properties of polyethylene pipes - Part 1: degradation of post yield mechanical properties and fracture surface analyses, *Polym. Degrad. Stabil.* 148 (2018) 75–85.
- [52] Suleyman Devenci, Nisha Antony, Sulistiyanto Nugroho, et al., Effect of carbon black distribution on the properties of polyethylene pipes Part 2: degradation of butt fusion joint integrity, *Polym. Degrad. Stabil.* 162 (2019) 138–147.
- [53] ISO 4427-1:2019 (E), Plastics Piping Systems for Water Supply and for Drainage and Sewerage under Pressure-Polyethylene (PE) Part 1:General.
- [54] ASTM F714-13, Standard Specification for Polyethylene (PE) Plastic Pipe (DR-PR) Based on outside Diameter, 2019.
- [55] Haroon Rashid, BUTT FUSION WELDING OF POLYETHYLENE PIPES [D], BRUNEL UNIVERSITY, 1997.
- [56] R.P. Wool, B.-L. Yuan, O.J. McGarel, Welding of polymer interfaces, *Polym. Eng. Sci.* 29 (19) (1989).
- [57] J. Liu, C. Yang, T. Yin, et al., Polyacrylamide hydrogels. II. elastic dissipater, *J. Mech. Phys. Solid.* 133 (2019) 103737.
- [58] Binhong Liu, Tenghao Yin, Jinye Zhu, et al., Tough and fatigue-resistant polymer networks by crack tip softening, *Proc. Natl. Acad. Sci. USA* 120 (6) (2023) e2217781120.